Application of the CRS stack to seismic data of Amazon paleozoic basin

German Garabito (*), João C. R. Cruz(*), Jaime Eiras (*) and Norcirio P. Queiroz (**)
(*) CPGF/UFPA/Brazil and (**) Petrobras

This paper was prepared for presentation at the 8th International Congress of The Brazilian Geophysical Society held in Rio de Janeiro, Brazil, 14-18 September 2003.

Abstract

A problem frequently encountered in petroleum exploration of the Solimões and Amazon basins in Brazil is the presence of igneous rocks, e.g. diabase sills, intruded in the Paleozoic sequences. Diabase sills reduce the seismic imaging quality because they cause low signal-to-noise ratio, multiple reflections, and spherical divergence. They can also mislead the interpretation by creating false structures due to pull-up effect. The development of modern seismic processing techniques and re-processing of seismic data are proposed to solve this kind of problem. In this paper we present a new stack method, namely Common-Reflection-Surface (CRS), that simulates zero-offset (ZO) sections and as by-product gives new kinematic wavefield attributes. Unlike the conventional Normal-Moveout/Dip-Moveout (NMO/DMO) stack, the CRS stack provides higher resolution and does not depends on the macro-velocity model. In this paper, we apply successfully the CRS stack to a seismic data set of the Amazon paleozoic basin.

Introduction

The presence of igneous rocks intruded into sedimentary layers consists a serious problem for the petroleum exploration. We find many examples in the specialized literature where due to the high impedance contrast in the overburden, it is not possible to obtain a good seismic image of the target structure. In Brazil we have basalt layers in the Paraná basin and diabase sills in the Amazon paleozoic basins.

In the Amazon region, object of this paper, these problems can be summarized as follows:

1. Signal-to-noise decreases and multiples reflections occur specially when a high-velocity diabase sill lies just below the Paleozoic-Cretaceous unconformity due to the high-impedance contrast.
2. Diffraction effects and velocity anomalies (pull-down) can appear in areas intensively fractured by tectonics related to the igneous activity.
3. Diffraction and pull-up effects can occur due to anomalous thickening or jumping of the diabase bodies.
4. Lateral velocity anomalies, diffractions, pull-up, and consequent false structures can occur at diabase sill edges.

An illustrative example of these situations is shown in Figure 1, based on the geological model for the Amazon basin.

During the Sub-Basalt Imaging Conference carried out by the University of Cambridge, UK, April, 2002, many new ideas and techniques were proposed to improve the seismic imaging quality beneath the high impedance layers. Trape et al. (2002) presented a successful application of the CRS stack method to real data set.

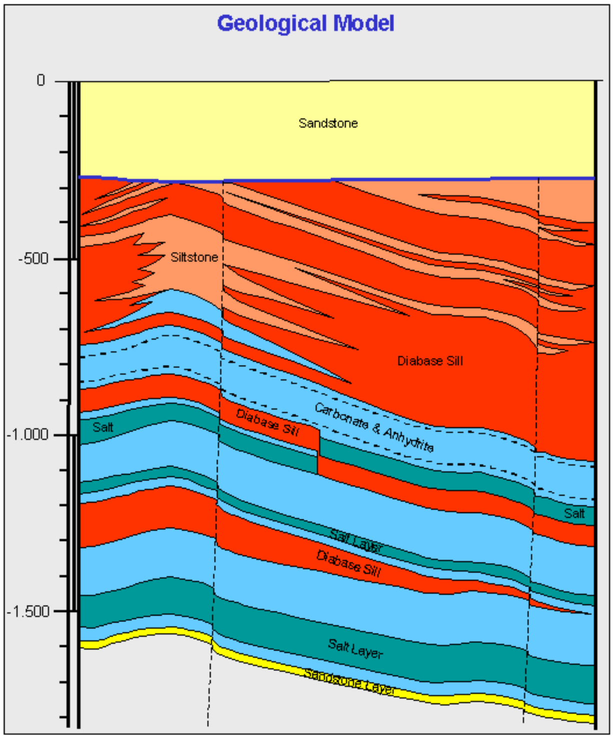

Figure 1: Geological model of the Amazon region paleozoic basin.

The CRS stack method (Jäger et al., 2001; Garabito et al. 2001a) provides a high-resolution ZO section and useful wavefield kinematic attributes. The necessary assumption about earth model is that it must satisfy all the conditions of the zero-order ray theory approach. It is not necessary any velocity analysis in this method, so that they are referred to as "macro-model-independent method" (Hubral, 1999). For applying it we have to know a near-surface wavefield velocity. The CRS method deserves to simulate ZO sections from multi-coverage seismic data (see e.g., Müller, 1999; Mann et al., 1999; Jäger et al., 2001; Garabito, et al. 2001a, 2001; Biloti, 2001) with sources and receivers located on a straight line (the seismic line) on the measurement surface. The CRS stacking operator is a traveltime surface derived by means of the second-order paraxial ray theory and is calculated by using a hyperbolic paraxial traveltime approach.

In this paper we do not emphasize theoretical aspects of the CRS stack method. For that we address the readers to the many works, e.g. Hubral (1999), Müller, 1999, and Garabito (2001). Here the main goal is to show an application of the CRS stack as a tool to improve the seismic imaging quality. For this, in framework of the project "Seismic imaging of diabase sills in the Amazon region paleozoic basins", that was supported by CTPETRO/FINEP/PETROBRAS/UFPA Convey, we chose a seismic data set of the north ramp of the Amazon basin. The result of the CRS stack was an enhanced image of the structure below the high impedance layers, in comparison to the conventional NMO/DMO stack method.

CRS Stack Method

To simulate a ZO section by CRS method, we stack the data along the stacking operator and assign the stacked value to a point $P_o(x_o, t_o)$ of the ZO section to be simulated. The normal ray emerges at a central point with horizontal coordinate x_o, and reflection traveltime t_o. For 2-D media, this operator depends on three parameters, which are associated with two hypothetical waves, namely the normal-incidence-point (NIP) and Normal (N) waves (Hubral, 1983). These parameters are the emergence angle of the normal ray, β_0, and two wavefront curvatures, K_{NIP} and K_N, of the NIP and N waves, respectively. The best parameter triplet is determined in sense of the maximum semblance (objective function) value obtained at the point $P_o(x_o, t_o)$ of the ZO section to be simulated. The CRS stack results are: 1) High resolution ZO section; 2) maximum coherence section; 3) radius of curvature of the NIP wave; 4) radius of curvature of the Normal wave; and 5) emergence angle of the normal ray.

The CRS stack strategy used in this paper follows Garabito et al. (2001a), that is summarized into the three steps:

Step I: Pre-Stack Global Optimization

The multi-coverage pre-stack seismic data is the input. The inverse problem is stated to estimate the best β_0 and $R_{NIP} = 1/K_{NIP}$ with the maximum semblance value. The results of this step are: 1) maximum coherence section, 2) emergence angle β_0 section, 3) radius of curvature of NIP wave section, and 4) simulated ZO section. In this step, the used CRS operator is a reduced form by using the condition $K_{NIP} = K_N$.

Step II: Post-Stack Global Optimization

The post-stack seismic data is the input. The inverse problem is stated to estimate the parameter $R_N = 1/K_N$ corresponding to the maximum semblance, by fixing the angle β_0 obtained in the previous step. In this step the main result is a radius of curvature of N wave section.

Step III: Pre-Stack Local Optimization

The pre-stack multi-coverage seismic data is the input. The inverse problem is stated to estimate the best triplet parameter (β_0, R_{NIP}, R_N) with the maximum semblance. In this step the results are: 1) maximum coherence section, 2) emergence angle β_0 section, 3) radius of curvature of NIP wave section, 4) radius of curvature of N wave section, and 5) simulated ZO section.

The first two steps are carried out using a simulated annealing (SA) algorithm for global optimization. At the third step we used a quasi-Newton method for local optimization.

All three steps are important for the final result. The first two steps deserve to search for a good initial approximation, while it is at the third step that we refine the estimated parameter triplet and obtain an improved ZO section.

Near-Surface Layer

By considering land seismic data, in general, the reflection time observations are affected by irregularities in the near-surface, namely changes in elevation, base of weathering, and weathering velocity. All these factors can be included in the CRS stack formalism. The interested readers are addressed to the works of Chira et al. (2001), and Chira and Hubral (2003).

In this paper we consider the existence of a planar horizontal measurement surface, and a homogeneous near-surface layer. In case of land seismic data, it is applied a pre-processing step consisting of the conventional static correction referenced to a known datum, e.g. the relative sea level (RSL). The picking phase and uncertainty of the weathering velocity contribute to reduce the accuracy of the CRS parameter estimates, nevertheless high resolution and consistency remain as features of the CRS stacked section. In this paper, we consider a constant near-surface velocity equals 1700 m/s, which corresponds to the velocity just beneath the static RSL.

Seismic Data Analysis

In the Figure 2, we show an example of the registered seismic data. It consists of a split-spread shot record with low signal-to-noise ratio. It is a feature of this record the presence of ground roll energy, which is characterized by low-frequency, high-amplitude appearance and contamination of short-offsets. This kind of energy is found in the shot records along all seismic line. Besides, the seismic amplitudes after 1.5 second are strongly contaminated and do not yield any possibility to define reflection horizons.

For the CRS stack application in this paper we focused the time interval until 1.0 second in the ZO section, and a distance from the first to the last simulated trace of 12000 m.

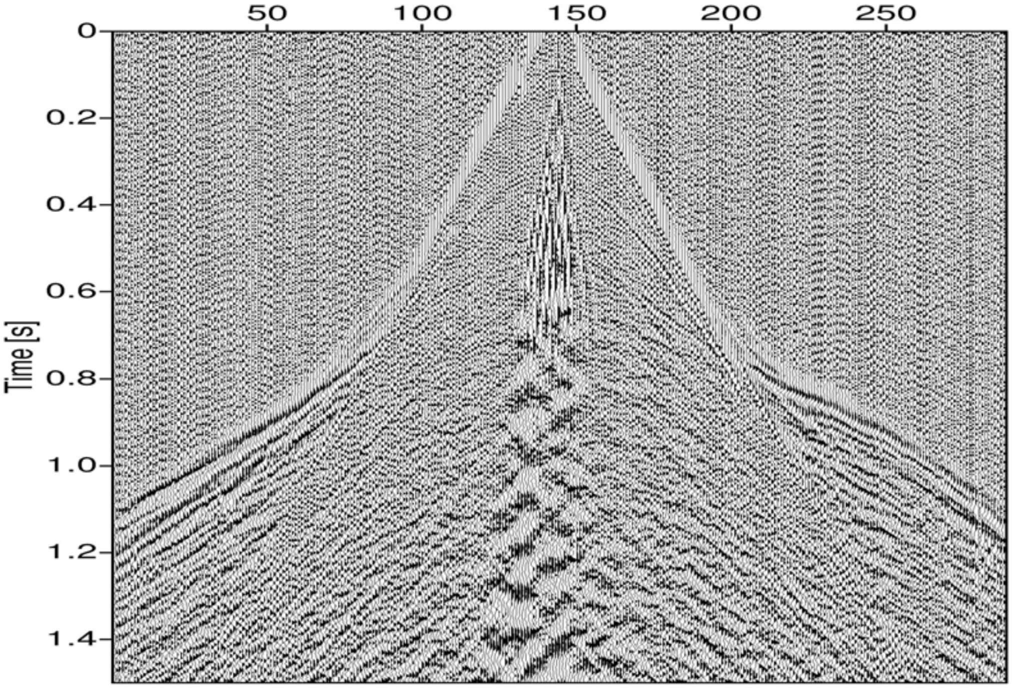

Figure 2: Shot record of the seismic line in the north ramp of the Amazon paleozoic basin.

CRS Stack Pre-Processing

Before applying the CRS stack the seismic data must be submitted to the final static correction for avoiding irregularities in the near-surface layer. Afterwards, a surface consistent deconvolution was applied. In order to attenuate the ground roll energy the data set must be (ω, k)-filtered. The Figure 2 is an example of the pre-processed common shot section. Before starting the CRS stack algorithm, it should be considered a stack aperture analysis. For this, some a priori information about the CRS stack parameters must be introduced.

CRS Stack Processing

By using some physical constraints, we should define intervals for each parameter to be searched-for.

The first step was carried out using the all multi-coverage data. The CRS stack operator was constructed under the diffraction condition $K_{NIP} = K_N$.

The second step was carried out using the previous simulated ZO section as input, with 281 seismic traces. The CRS stack operator was constructed by considering $h = 0$.

The third step was performed using the multi-coverage data. Here, it was used the full CRS operator, that depends on the parameter triplet (K_{NIP}, K_N, β_o).

At each step, the semblance function is evaluated for each point of the ZO section to be simulated. This means that we have an evaluated ZO section related to the best parameters estimated by the optimization process. It is important to emphasize that the first two steps use a global optimization performed by SA algorithm, and the third step uses a local optimization by quasi-Newton method. By global optimization the CRS stack algorithm is able to find more than one maximum for the objective function. This is an important feature to solve conflicting dip problems. As shown in Garabito et al. 2001b, both maxima must be considered for stacking in case of conflicting dips, in order to simulate correctly the seismic event. In the other hand, the local optimization is important to refine the simulated ZO seismic section.

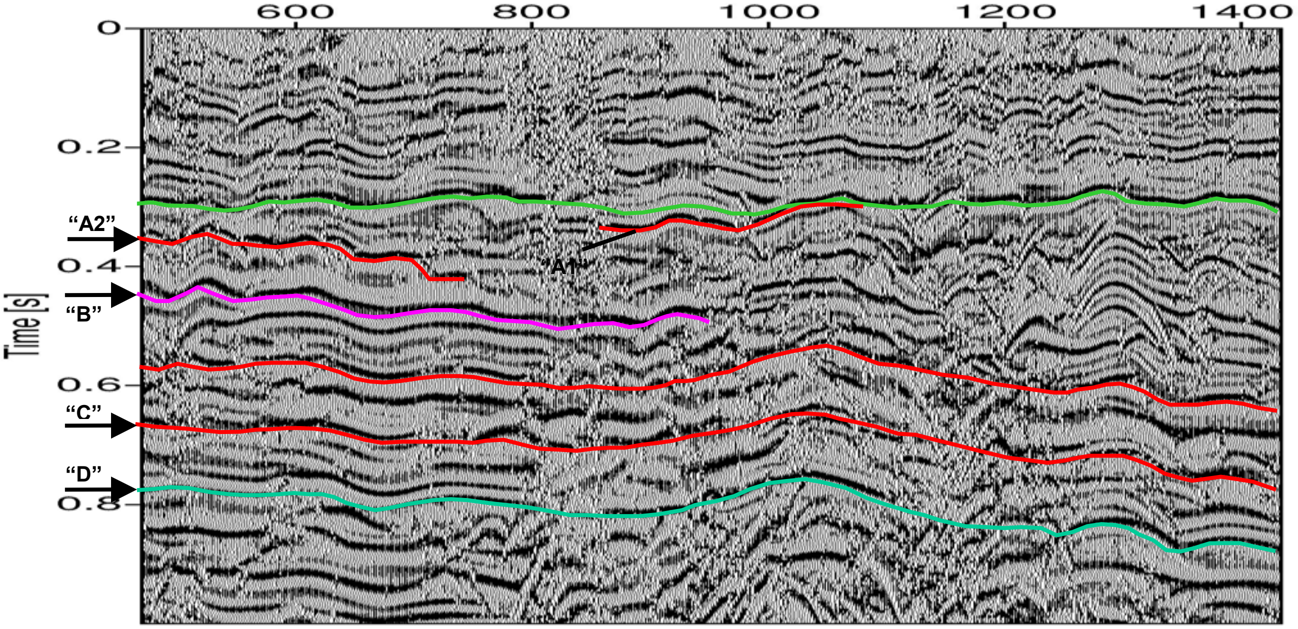

Figure 3: ZO seismic section simulated by the CRS stack method.

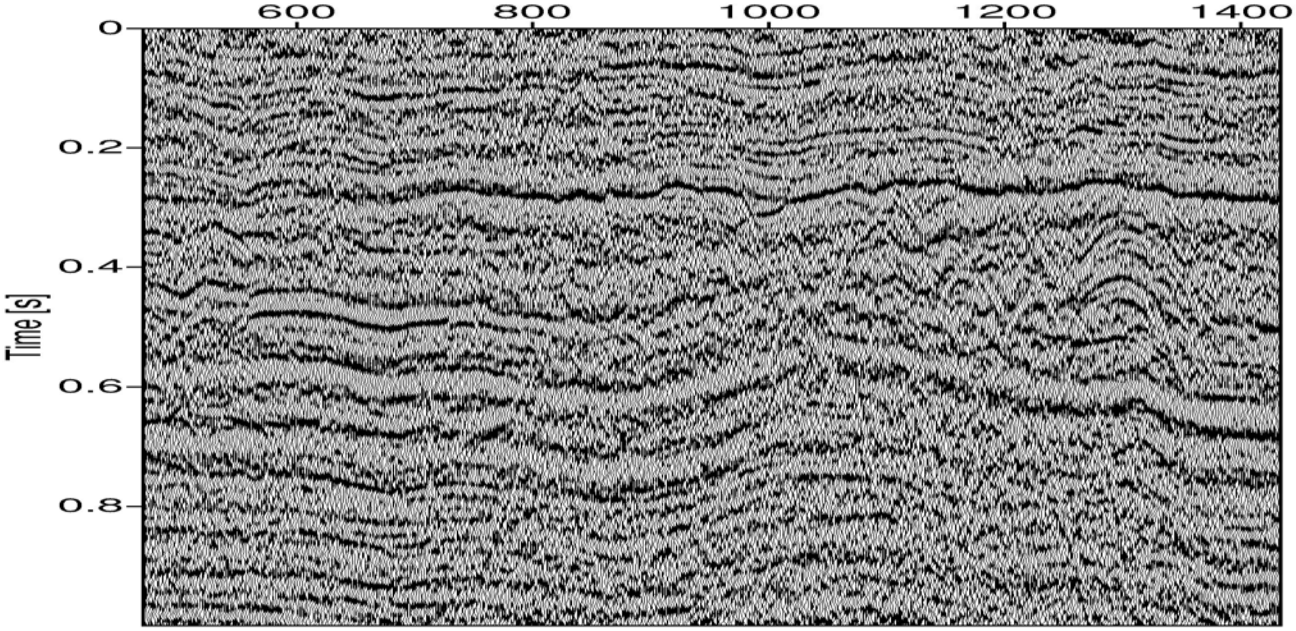

Figure 4: ZO seismic section simulated by the NMO/DMO stack method.

Application of the CRS Stack

Figure 3 shows the result of the CRS stack application and the Figure 4 is the results of the NMO/DMO stacked section. In general, the CRS stack process improves the simulated ZO section because it considers larger number of seismic traces for stacking. The dipping reflectors and structures images are enhanced in the CRS stacked section, because its formalism considers dip effects and curvatures.

The simulated ZO section includes multiple events, which must be considered by additional processing by using the estimated CRS parameters.

The seismic reflector (A) of the ZO section simulated by CRS stack (Figure 3) is better visualized than by

NMO/DMO stack (Figure 4). It is very irregular in shape, as well the overlying sequence.

By applying the CRS stack process the reflectors of the sequence between (B) and (C) are better defined than by using NMO/DMO stack.

A noisy strip near the center of the seismic line in the CRS stacked section can be related to a collapse zone possibly due to tectonic movements, as we can see in the Figure 3 by the reflection horizon (D).

Conclusions

We have applied successfully the CRS stack method to a seismic data set of the Amazon paleozoic basin in Brazil. The CRS stacked shows an improved simulated ZO section in comparison with the NMO/DMO stack, due to the CRS stack considers a larger number of seismic traces for stacking. The structure seismic imaging is enhanced in the CRS stack, because its formalism incorporates dip effects and curvatures. The estimated CRS parameters can be used for interval velocity determination and multiple corrections

Acknowledgments

We gratefully acknowledge the permission of the Petrobras to present their data. We thank CTPETRO/FINEP and PETROBRAS for supporting the project IMAGAM. The third author would like to thank to National Petroleum Agency (ANP/PRH/06) for supporting him as visiting researcher at UFPA.

References

Chira, P., and Hubral, P. 2003. Traveltime formulas of near-zero-offset primary reflections for a curved 2-D measurement surface: Geophysics, 68, no. 1, 255-261.

Chira, P., Tygel, M., Zhang, Y., and Hubral, P. 2001. Analytic CRS Stack formula for a 2D curved measurement surface and finite-offset reflections: Journal of Seismic Exploration, 5, no. 10, 245-262.

Garabito, G., Cruz, J. C. R. , Hubral, P. and Costa, J. 2001a. Common reflection surface stack by global optimization: 71th Annual Internat. Mtg., Soc. Expl. Geophys. Expanded Abstracts.

Garabito, G., Cruz, J. C. R. , Hubral, P. and Costa, J. 2001b. Empilhamento de superfícies de reflexão comum com mergulhos conflitantes (in portuguese): 7th International Congress of Brazilian Geophysical Society. Expanded Abstracts.

Garabito, G., 2001. Empilhamento Sísmico por Superfície de Reflexão Comum: um novo algoritmo usando Otimização Global e Local (in portuguese): PhD thesis, Federal University of Para (Brazil).

Hubral, P. 1983. Computing true amplitude reflections in a laterally inhomogeneous earth: Geophysics, 48, no. 8, 1051-1062.

Hubral, P., Ed., 1999, Macro-model independent seismic reflection imaging, volume 42, J. Appl. Geophys.

Jäger, R., Mann, J., Höcht, G., and Hubral, P., 2001. Common-reflection-surface stack: Image and attributes: Geophysics, 66, no 1, 97-109.

Mann, J., Jäger, R., Müller, T., Höcht, G. and Hubral, P. 1999, Common-reflection-surface stack – a real data example: J. Appl. Geoph., 42, no.3,4, 301-318.

Müller, T., 1999. The common reflection surface stack – seimic imaging without explicit knowledge of the velocity model: Der Andere Verlag, Bad Iburg.

Trappe, H.; Pruessmann, J.; and Gierse, G., 2002, Improved imaging below high-impedance sediments by Common-Reflection-Surface (CRS) stack. Journal of Conference Abstracts, Vol. 7(2). Sub-Basalt Imaging Conference, Cambridge, UK.

Zhang, Y., Höcht, G., and Hubral, P. 2002. 2D and 3D ZO CRS stack for a complex top-surface topography: 64th Annual Internat. Mtg., Eur. Assoc. Expl. Geophys., Extended Abstracts.